Gpr125 Plays Critical Roles in Lacrimal Myoepithelia and Tear Film

Departments of Cell Biology[1] Dermatology[2] and Ophthalmology[3]

New York University School of Medicine

Elena Spina[1], Rebecca Handlin[1], Julia Simundza[1], Angela Incassati[1], Muneeb Faiq[3], Anoop Sainulabdeen[3], Kevin C Chan[3], Pamela Cowin[1,2]*

*Address for correspondence:

Dr. Pamela Cowin

New York University Medical Center

MSB 621, 550 1st Ave

New York, NY 10016

E-mail: pamela.cowin@nyulangone.org

Conflict of interest statement: The authors declare that no conflict of interest exists.

Abstract

Gpr125, encoded by *Adgra3*, is an orphan adhesion G-protein coupled receptor (aGPCR) implicated in Wnt signaling and planar polarity. Here we establish both physiological and pathological roles for Gpr125. We show that mice lacking Gpr125 display an ocular phenotype with many hallmarks of human dry eye disease. These include squinting, abnormal lacrimation, mucus accumulation, swollen eyelids and inflammatory infiltration of lacrimal and meibomian glands. We further demonstrate that mice expressing Gpr125 lacking six transmembrane and the cytoplasmic domain recapitulate the null phenotype, indicating that downstream signaling is essential. Utilizing a Gpr125-β-gal reporter and scRNAseq, we identify Gpr125 expression in a discrete population of embryonic myoepithelial cells located at the tips of developing lacrimal ducts. By lineage tracing we show these cells function as progenitors of the adult lacrimal myoepithelium. Beyond defining an essential role for Gpr125 in tear film and identifying its utility as a marker of lacrimal progenitors, this study implicates Gpr125 in the etiology of dry eye disease, and defines novel animal models of this common malady.

Introduction

Tears are required to lubricate corneal and conjunctival surfaces and to prevent eyes from desiccation (1). They also function to protect eyes from microbial infection and preserve visual acuity. Dry Eye Disease (DED) is a significant health problem that is particularly prevalent in the elderly and women (2-4). It affects ~5% of the population overall and is a central feature of Sjogren's syndrome, the third most common auto-immune disease (2-4).

Tear film is composed of three layers, each secreted from a different source. Goblet cells, clustered along the conjunctival rim, provide the inner mucus layer that spreads tear film evenly over the ocular surface (5). Meibomian glands, found between eyelash follicles on the inner surface of eyelids, produce the outer lipid layer that prevents evaporation (6). Lacrimal glands, secrete the central aqueous component that contains water-soluble immuno-active and antibacterial proteins, as well as glucose, urea, and salts (7). Defects in the volume or composition of any layer destabilizes tear film and induces DED.

Like other ectodermal appendages, lacrimal and meibomian glands develop during mid-embryogenesis. Murine lacrimal glands emerge around embryonic day 13 (E13) as a bulbous outgrowth of the conjunctival epithelium, which by E15 has elongated as a bi-layered hollow duct with 4-5 bulbous tips. Subsequent branching produces a compact mass of secretory acini, enmeshed by contractile myoepithelial cells, which fully differentiate after birth (7-10). Meibomian glands emerge ~E18 as a row of placodes along the margins of the inner eyelids (11). These invaginate as solid chords, form lumen

around postnatal day 3 (P3), then branch ~P5 and complete acinar differentiation ~P8-15 (11). Goblet cells appear in the conjunctival rim coincident with eye opening (5, 12).

Analysis of knockout (KO) mice has revealed a suite of critical regulators of tear film (5, 7-9, 13-20). However, the involvement of GPCRs in this process has not been studied. Here we uncover an essential physiological role for Gpr125 in tear film, and a pathological role in the etiology of DED. Gpr125 was discovered through homology searches of the human genome database and is an orphan aGPCR (21). Like other members of this family, Gpr125 has a large extracellular domain with sequence similarity to cell adhesion molecules (**Figure 1A**). It remains unclear, however, if it functions in cell adhesion or signals via G-proteins (21, 22). Previous studies have highlighted Gpr125 as a marker of undifferentiated murine spermatogonial progenitors (23), documented its elevation in the choroid plexus following injury and correlated its high expression with both good and poor outcome in cancer (24-26). Ectopic expression of Gpr125 has shown that in zebrafish it modulates Wnt/planar cell polarity processes by interacting with the cytoplasmic adaptor Disheveled (Dsh), and in cultured cells undergoes constitutive clathrin-mediated internalization to endosomes (27, 28). However, the physiological function of native Gpr125 has remained elusive.

Combined Results & Discussion

Mice lacking Gpr125 display blepharitis, blepharedema and mucoid accumulation. To address the role of native Gpr125, we developed mice that permit Gpr125 expression to be ablated and the lineage of cells normally expressing it to be traced by inserting a creER^{T2} cassette downstream of the *Adgra3* promoter (**Figure 1B**). Mice lacking Gpr125 expression (*Adgra3*$^{cre/cre}$) display a prominent eye phenotype (**Figure 1C**) comprising several hallmarks of DED. *Adgra3*$^{cre/cre}$ mice squint as soon as their eyes open; whereas, heterozygous *Adgra3*$^{cre/+}$ are indistinguishable from wild-type littermates (**Figure 1C**). As *Adgra3*$^{cre/cre}$ mice mature, this early blepharitis progresses to blepharedema (swollen balding eyelids) and mucus precipitation (**Figure 1D**). The phenotype is constant in males but in females oscillates with reproductive status, becoming pronounced during pregnancy and lactation. During these stages, mice develop proptosis (bulging eyes) that resolves during weaning. The eye phenotype in *Adgra3*$^{cre/cre}$ mice is 100% penetrant on all strain backgrounds examined (C57B6/CH3, FVBN, and mixed). To dissect the role of Gpr125's adhesion ectodomain from its internal signaling functions we examined a second strain, *Adgra3*$^{lz/lz}$, which expresses the Gpr125 ectodomain and 1st transmembrane domain fused in frame to β-galactosidase and lacks regions required for signaling/adaptor functions (**Figure 1E**) (23). Homozygous *Adgra3*$^{lz/lz}$ mice recapitulate the *Adgra3*$^{cre/cre}$ null phenotype (**Figure 1F**), whereas, *Adgra3*$^{lz/+}$ mice are normal. Collectively, these data demonstrate that Gpr125 has an essential physiological role in normal eye development and indicate that signaling downstream of the receptor is required. Our genetic analyses also reveal that loss of Gpr125 protein or Gpr125 signaling

is sufficient to trigger several common eye pathologies, such as blepharitis, blepharedema and mucoid accumulation.

Gpr125 in ciliary body and iris

Next we examined adult eye globes by X-gal staining and found strong Gpr125-β-gal expression in the ciliary body, which secretes aqueous humor, and in the inner layer of the iris of *Adgra3*$^{lz/+}$ mice (**Figure 2A, B**). As abnormal aqueous humor dynamics can alter intraocular pressure (IOP), which is a major risk factor for glaucoma, we measured IOP, but found no significant difference between wildtype and mutant genotypes (**Figure 2C**).

Goblet cell and meibomian pathologies

We submitted both strains for evaluation by a veterinary ophthalmologist. Examination of the lens and retina by slit lamp revealed well-documented characteristics of control B6 and FVBN mice, but no abnormality specifically linked to the *Adgra3*$^{cre/cre}$ or *Adgra3*$^{lz/lz}$ genotypes. Fluorescein staining found no evidence for corneal abrasion, but highlighted the presence of large mucoid precipitates around the eyelids of homozygous mutants (**Figure 2D**). This feature pointed towards abnormal tear film composition (**Figure 2E**), prompting us to investigate the tear glands in more detail. As *Adgra3* mutant mice had swollen eyelids we looked for changes in goblet cells and meibomian glands. Histological sections of eyelids stained with Alcian blue revealed goblet cell in *Adgra3*$^{cre/cre}$ mice (**Figure 2F**) but with greater variation in number (average =70/eyelid; range 7-210 n=23) compared to controls (average of 65 goblet cells/eyelid; range 45-94; n=23): some

showed epithelial and goblet cell desquamation next to swathes of mucus; others showed clusters of goblet cells. Meibomian glands displayed inflammatory infiltration by T-cells and macrophages (**Figure 2G,H**). Surprisingly, X-gal staining of eyelids indicated that goblet cells and meibomian glands were devoid of Gpr125 expression (**Figure 2I**), though eyelash follicles stained prominently, serving as internal procedural controls. These data show that changes in goblet and meibomian glands, reminiscent of symptoms accompanying human DED, occur in *Adgra3* mutants. However, they indicate that these changes are not the initiating event. Rather, they are the secondary abrasive consequences of loss of Gpr125 elsewhere.

$Adgra3^{cre/cre}$ and $Adgra3^{lz/lz}$ mice have abnormal lacrimation.

Next we tested whether Gpr125 loss affected the lacrimal function by measuring tear volume. $Adgra3^{cre/cre}$ and $Adgra3^{lz/lz}$ mice produced two to three-fold more tears than heterozygous or wild-type controls (**Figure 3A**). Tear volume was greater in female than male mice. $Adgra3^{cre/cre}$ and $Adgra3^{lz/lz}$ mice often presented (**Figure 3H**) with a mild phenotype in one eye (squint only) and a severe phenotype (blepharedema and or mucus) in the other. When we separated eyes into these two categories according to photographic assignment taken prior to measurement and reanalyzed the data, we found tear volume for the mild phenotypic category were similar, and sometimes lower, than those of wildtypes. In contrast, those in the severe category showed high values indicative of excessive tearing (**Figure 3A**). Thus, our mice recapitulated the paradoxical

phenomenon documented in human patients where individuals with tear film abnormality originating from initial ocular dryness respond with secondary hyper-lacrimation.

Adgra3$^{cre/cre}$ and *Adgra3*$^{lz/lz}$ mice show inflammatory infiltration of lacrimal glands

Inflammatory infiltration of lacrimal glands plays a significant role in the pathological mechanism of Sjogren's syndrome and is a frequent feature of sporadic DED (2-4, 29). To test if *Adgra3* mutant mice modeled this we examined histological sections of lacrimal glands and found foci, composed of small round cells, in both *Adgra3*$^{cre/cre}$ (**Figure 3B, S1**) and *Adgra3*$^{lz/lz}$ mice. Lack of immunostaining for cytokeratin5 (CK5) indicated that myoepithelial cells were lost in these regions (**Figures 3C,D**). The foci were surrounded by F480-positive macrophages (**Figures 3C,E**), and filled with cells recognized by CD4 and CD8 antibodies (**Figures 3C, F,G, S1**) indicating infiltration by T-helper cells and cytoxic T-cells. Histological analysis of females with facial swelling (**Figure 3H**) and proptosis during pregnancy and lactation revealed enlarged lacrimal glands (**Figure 3I,J**) and swathes of macrophages around large areas of acinar loss (**Figure 3K**). Thus, loss of Gpr125 predisposes the lacrimal gland to lymphocytic infiltration, replicating the inflammatory infiltration seen in human DED and the epidemiological characteristics seen in humans with respect to gender and reproductive status.

Gpr125-expressing cells are located at the leading tips of ducts during lacrimal development and function as progenitors of the lacrimal myoepithelium.

Given the significant effect of *Adgra3* mutation and loss on lacrimal structure and function, we sought to identify cell types that express Gpr125 over the course of lacrimal development. We began by mining scRNAseq data (10). Gpr125 mRNA was detected in a small cell population that co-expressed myoepithelial mRNAs: keratin 14, smooth muscle actin, and Sox10 (**Figure 4A**). This population was present during ductal elongation (E16) but diminished by P4 (data not shown) as acinar differentiation ensued. Next, we stained embryos with X-gal to look for Gpr125 expression (**Figure 4B**). Gpr125-β-gal appeared in the lacrimal bud as it emerged from the conjunctival rim ~E14, but by E15.5 it was restricted to a discrete population of cells located at the leading tips of lacrimal ducts and by P1 at the front of lacrimal branches. Intriguingly, during the course of these experiments we noted that Gpr125-β-gal was also expressed within a well-characterized "bulge" stem cell compartment of hair follicles and whiskers (**Figure 4B**) (30). This prompted us to ask if the embryonic Gpr125-positive cells functioned similarly as lacrimal progenitors. To test this, we performed lineage tracing by using the *creER*^{T2} cassette present in *Adgra3*^{cre} mice to activate expression of a lineage reporter. We labeled embryos harboring the ROSA-lox-STOP-lox-tdTomato reporters at E13-E15 by delivering tamoxifen to *Adgra3*$^{cre/cre}$ dams during mid-pregnancy. Lacrimal glands were harvested at 7 weeks and 6 months of age, cleared and analyzed by 3-D immunofluorescence confocal microscopy (**Figure 4C**). At 7 weeks after birth, we found tdTomato (tdT)-labeled cells with an elongated shape along the basal borders of ducts and with stellate

morphology enmeshing acini. These characteristics, together with their expression of CK5, identified them as contractile myoepithelial cells. A similar pattern was seen in glands from mice harvested at 6 months, indicating significant longevity of the original progenitor population (**Figures 4D,E**).

Collectively, these data support the concept that Gpr125 is expressed in cells at migrating tips of embryonic lacrimal ducts that function as long-lived unipotent progenitors of the ductal and acinar myoepithelium. This finding, taken together with previous reports where Gpr125 expression was used to isolate spermatogonial progenitors, suggests that Gpr125 could have utility in isolating lacrimal progenitors.

Gpr125 is essential for the generation of a functional tear film

Our results establish a physiological role for Gpr125 in the eye and show that loss of this aGPCR induces many features of DED (**Figure 1**). Human DED results from tear film instability exposing the eye to irritation and desiccation, prompting compensatory excessive tearing and immune response, which leads to further lacrimal destruction. Our *Adgra3* mutants provide a new model that reproduces this complex spectrum of symptoms, from early eye discomfort to blepharedema (**Figure 1**), mucus accumulation **(Figures 1, 2D),** compensatory hyper-lacrimation, inflammatory infiltration of meibomian **(Figures 2H)** and lacrimal glands **(Figure 3B-G),** and goblet cells desquamation **(Figure 2F).** Moreover, *Adgra3* mutants show worsening of their eye phenotype during pregnancy

and lactation, recapitulating the hormonal/gender epidemiology of DED, which is more prevalent in women and exacerbated by pregnancy and post-menopause.

Many genetic mouse models of DED arise from immune dysregulation or defects in matrix inhibition of immune activation and thus recapitulate late stages of DED. In contrast, our mice identify an initiating event during lacrimal development that predisposes mice to the full pathophysiological progression of DED. Our data reveal that a discrete myoepithelial subpopulation of embryonic cells located at tips of ducts and branches express Gpr125, and function as unipotent progenitors of the lacrimal myoepithelium (**Figure 4**). Importantly, we show that in the absence of Gpr125, focal areas of the lacrimal gland become devoid of myoepithelium **(Figure 3D)** and infiltrated by lymphocytes and macrophages (**Figure 3B-G**). Our results support a critical role for myoepithelial cells in DED, and complement previous studies, which have shown that myoepithelial differentiation and contractile function is altered in Sjogren's patients (31, 32). It will be important to determine whether the phenotypes of *Adgra*3$^{cre/cre}$ and *Adgra3*$^{lz/lz}$ mice arise from defective myoepithelial adhesion, premature progenitor exhaustion, or impaired myoepithelial differentiation and matrix secretion.

Our mouse genetic results raise the question whether Gpr125 and its downstream pathways are involved in the etiology of human DED. If so, then *Adgra3*-KO mice will provide a powerful tool to study the pathological mechanism and progression of DED and to test therapeutic strategies to cure or manage DED. GPCRs are attractive candidates

for drug development and currently are targets of approximately 34% of drugs approved by the US Food and Drug Administration. Though less well understood, recent discoveries of involvement of aGPCRs in human disease has produced a growing interest in their therapeutic potential (33). Although Gpr125 is an orphan receptor evidence has emerged recently suggesting a role in receptor trafficking and endosomal signaling (28). Deciphering Gpr125 signaling pathways holds promise to uncover novel targets for therapeutic intervention in this common condition.

Methods: Refer to Supplemental Methods for details.

Study Approval: Animal experiments were approved by NYUMC institutional animal care and use committee and conformed to American Association for Accreditation of Laboratory Animal Care guidelines.

Statistics: Experimental data are presented as mean ± SEM. P values for experiments comparing two groups were calculated using student's t test. For experiments comparing more than two groups, an Ordinary one-way ANOVA was used with multiple comparisons test. $P<0.05$ was considered statistically significant.

Author Contributions: PC conceived the study, designed experiments and wrote the paper with input from ES and RB; ES RB JS AI MF and AS conducted the experiments.

Acknowledgements: This work was supported by Department of Defense W81XWH-17-1-0013 BC160959 (PC), NIH training grants: T32GM066704 (JS), T32CA009161-44 (AI) and The Susan G Komen Foundation For The Cure (AI). Histology and scRNAseq services were provided by the Applied Bioinformatics and Experimental Pathology Research Cores: Grants P30CA016087 and S10 OD021747. We thank Dr. Aris Economides, Regeneron, Tarrytown NY for advice on *Adgra3*creER^{T2} construction and Dr. Michael Brown DVM (Oradell Veterinary Center, NJ) for ophthalmological evaluation.

REFERENCES

1. Botelho SY. Tears and the Lacrimal Gland. *Sci Am.* 1964;211:78-86.
2. Schaumberg DA, Sullivan DA, and Dana MR. Epidemiology of dry eye syndrome. *Adv Exp Med Biol.* 2002;506(Pt B):989-98.
3. Schaumberg DA, Sullivan DA, Buring JE, and Dana MR. Prevalence of dry eye syndrome among US women. *Am J Ophthalmol.* 2003;136(2):318-26.
4. Pflugfelder SC, and de Paiva CS. The Pathophysiology of Dry Eye Disease: What We Know and Future Directions for Research. *Ophthalmology.* 2017;124(11S):S4-S13.
5. Gipson IK. Goblet cells of the conjunctiva: A review of recent findings. *Prog Retin Eye Res.* 2016;54:49-63.
6. Bron AJ, and Tiffany JM. The meibomian glands and tear film lipids. Structure, function, and control. *Adv Exp Med Biol.* 1998;438:281-95.
7. Makarenkova HP, Ito M, Govindarajan V, Faber SC, Sun L, McMahon G, et al. FGF10 is an inducer and Pax6 a competence factor for lacrimal gland development. *Development.* 2000;127(12):2563-72.
8. Dean C, Ito M, Makarenkova HP, Faber SC, and Lang RA. Bmp7 regulates branching morphogenesis of the lacrimal gland by promoting mesenchymal proliferation and condensation. *Development.* 2004;131(17):4155-65.
9. Dean CH, Miller LA, Smith AN, Dufort D, Lang RA, and Niswander LA. Canonical Wnt signaling negatively regulates branching morphogenesis of the lung and lacrimal gland. *Dev Biol.* 2005;286(1):270-86.
10. Farmer DT, Nathan S, Finley JK, Shengyang Yu K, Emmerson E, Byrnes LE, et al. Defining epithelial cell dynamics and lineage relationships in the developing lacrimal gland. *Development.* 2017;144(13):2517-28.
11. Nien CJ, Massei S, Lin G, Liu H, Paugh JR, Liu CY, et al. The development of meibomian glands in mice. *Mol Vis.* 2010;16:1132-40.
12. Rios JD, Forde K, Diebold Y, Lightman J, Zieske JD, and Dartt DA. Development of conjunctival goblet cells and their neuroreceptor subtype expression. *Invest Ophthalmol Vis Sci.* 2000;41(8):2127-37.
13. Tsau C, Ito M, Gromova A, Hoffman MP, Meech R, and Makarenkova HP. Barx2 and Fgf10 regulate ocular glands branching morphogenesis by controlling extracellular matrix remodeling. *Development.* 2011;138(15):3307-17.
14. Chen Z, Huang J, Liu Y, Dattilo LK, Huh SH, Ornitz D, et al. FGF signaling activates a Sox9-Sox10 pathway for the formation and branching morphogenesis of mouse ocular glands. *Development.* 2014;141(13):2691-701.
15. Kenchegowda D, Swamynathan S, Gupta D, Wan H, Whitsett J, and Swamynathan SK. Conditional disruption of mouse Klf5 results in defective eyelids with malformed meibomian glands, abnormal cornea and loss of conjunctival goblet cells. *Dev Biol.* 2011;356(1):5-18.
16. Marko CK, Menon BB, Chen G, Whitsett JA, Clevers H, and Gipson IK. Spdef null mice lack conjunctival goblet cells and provide a model of dry eye. *Am J Pathol.* 2013;183(1):35-48.

17. Tong L, and Gupta PK. Need for Animal Models of Meibomian Gland Dysfunction. *Ophthalmol Ther.* 2016;5(2):129-34.
18. Plikus M, Wang WP, Liu J, Wang X, Jiang TX, and Chuong CM. Morpho-regulation of ectodermal organs: integument pathology and phenotypic variations in K14-Noggin engineered mice through modulation of bone morphogenic protein pathway. *Am J Pathol.* 2004;164(3):1099-114.
19. Cui CY, Smith JA, Schlessinger D, and Chan CC. X-linked anhidrotic ectodermal dysplasia disruption yields a mouse model for ocular surface disease and resultant blindness. *Am J Pathol.* 2005;167(1):89-95.
20. McMahon A, Lu H, and Butovich IA. A role for ELOVL4 in the mouse meibomian gland and sebocyte cell biology. *Invest Ophthalmol Vis Sci.* 2014;55(5):2832-40.
21. Bjarnadottir TK, Gloriam DE, Hellstrand SH, Kristiansson H, Fredriksson R, and Schioth HB. Comprehensive repertoire and phylogenetic analysis of the G protein-coupled receptors in human and mouse. *Genomics.* 2006;88(3):263-73.
22. Simundza J, and Cowin P. Adhesion G-protein-coupled receptors: elusive hybrids come of age. *Cell Commun Adhes.* 2013;20(6):213-26.
23. Seandel M, James D, Shmelkov SV, Falciatori I, Kim J, Chavala S, et al. Generation of functional multipotent adult stem cells from GPR125+ germline progenitors. *Nature.* 2007;449(7160):346-50.
24. Pickering C, Hagglund M, Szmydynger-Chodobska J, Marques F, Palha JA, Waller L, et al. The Adhesion GPCR GPR125 is specifically expressed in the choroid plexus and is upregulated following brain injury. *BMC Neurosci.* 2008;9:97.
25. Wu Y, Chen W, Gong L, Ke C, Wang H, and Cai Y. Elevated G-Protein Receptor 125 (GPR125) Expression Predicts Good Outcomes in Colorectal Cancer and Inhibits Wnt/beta-Catenin Signaling Pathway. *Med Sci Monit.* 2018;24:6608-16.
26. Fu JF, Yen TH, Chen Y, Huang YJ, Hsu CL, Liang DC, et al. Involvement of Gpr125 in the myeloid sarcoma formation induced by cooperating MLL/AF10(OM-LZ) and oncogenic KRAS in a mouse bone marrow transplantation model. *Int J Cancer.* 2013;133(8):1792-802.
27. Li X, Roszko I, Sepich DS, Ni M, Hamm HE, Marlow FL, et al. Gpr125 modulates Dishevelled distribution and planar cell polarity signaling. *Development.* 2013;140(14):3028-39.
28. Spiess K, Bagger SO, Torz LJ, Jensen KHR, Walser AL, Kvam JM, et al. Arrestin-independent constitutive endocytosis of GPR125/ADGRA3. *Ann N Y Acad Sci.* 2019;1456(1):186-99.
29. Pflugfelder SC, Bian F, Gumus K, Farley W, Stern ME, and De Paiva CS. Severity of Sjogren's Syndrome Keratoconjunctivitis Sicca Increases with Increased Percentage of Conjunctival Antigen-Presenting Cells. *Int J Mol Sci.* 2018;19(9).
30. Cotsarelis G, Sun TT, and Lavker RM. Label-retaining cells reside in the bulge of the pilosebaceous unit: implications for follicular stem cells, hair cycle, and skin carcinogenesis. *Cell.* 1990;61:1329-37.
31. Hawley D, Tang X, Zyrianova T, Shah M, Janga S, Letourneau A, et al. Myoepithelial cell-driven acini contraction in response to oxytocin receptor stimulation is impaired in lacrimal glands of Sjogren's syndrome animal models. *Sci Rep.* 2018;8(1):9919.

32. Makarenkova HP, and Dartt DA. Myoepithelial Cells: Their Origin and Function in Lacrimal Gland Morphogenesis, Homeostasis, and Repair. *Curr Mol Biol Rep.* 2015;1(3):115-23.
33. Bassilana F, Nash M, and Ludwig MG. Adhesion G protein-coupled receptors: opportunities for drug discovery. *Nat Rev Drug Discov.* 2019;18(11):869-84.

SUPPLEMENT

MATERIALS AND METHODS

Mice: Mice were constructed by Ingenious Technologies, Ronkonkoma, NY as follows. A cassette containing *CreER*^{T2} followed by a 3' polyadenylation signal, harboring SV40-driven Neo flanked by FRT sites inserted in a central intron, was recombined into a bacterial artificial chromosome (BAC) to place *CreER*^{T2} under the control of the *Adgra3* promoter, excising 502 bp encompassing 221 bp of exon 1 and part of the following intron 1-2 of *Adgra3*. Mice generated from these ES cells were selected for germline transmission by PCR, verified by southern analysis and sequencing then bred to a Flp deleter strain to remove Neo. *Adgra3*$^{lz/+}$ mice were generated by Regeneron using VelociGene methods (Valenzuela, D.M. et al. High-throughput engineering of the mouse genome coupled with high-resolution expression analysis. Nat Biotechnol 21, 652-659 (2003) to modify a bacterial artificial chromosome (BAC) clone carrying the mouse *Adgra3* gene by replacement of sequence encompassing exons 16-19 with *lacZ* to produce expression of fusion protein comprising the N-terminal extracellular domain, the first transmembrane domain, and part of the first intracellular loop of Gpr125 fused to β-galactosidase (Figure 1A) (23).

Ophthalmologic examination: Standard ophthalmic examination was performed by a trained veterinary ophthalmology consultant (Dr. Michael Brown, Oradell Veterinary Center, New Jersey). Slit lamp biomicroscopy was used to assess the cornea, anterior

chamber, iris, lens, and vitreous humor. Mydriasis was induced with tropicamide and the retina was examined via indirect ophthalmoscopy.

Corneal fluorescein staining was performed by applying sodium fluorescein (1%), for 3 minutes to the cornea of mice. Excess fluorescein was removed by flushing with sterile phosphate buffered saline (PBS) and corneal staining was evaluated and photographed with a slit lamp biomicroscope (Humphrey-Zeiss, Dublin, CA) using a cobalt bluelight. Punctate staining was recorded using a standardized National Eye Institute grading system of 0 to 3 for each of the five areas of the cornea.

Schirmer Tear Test: Tear production was measured via a modified Schirmer Tear Test. Briefly, 35mm x 5mm wide commercial Schirmer Tear Test standardized sterile strips (Schirmer Tear Test; Merck Animal Health) were transected with into two 15mm x 2.5mm strips, with the top notch removed. Individual strips were placed under the lower eyelid using forceps and removed after 15 seconds. The length of dye migration and wetting of the strip was measured in millimeters under a dissecting microscope.

Intraocular pressure measurement

Mice were anesthetized and maintained on isoflurane through a nose cone. IOPs were measured using a TonoLab rebound tonometer (Icare, Finland) within 5 min after isoflurane gas anesthesia induction. For every 6 valid measurements, the highest and lowest IOP values were automatically excluded by the device, and the average of the remaining 4 IOP values was displayed along with the deviation. For quality control, only

averages with slight deviation of less than 2.5 mmHg were considered acceptable readings. This procedure was repeated at least 3 times for each eye, and the acceptable readings were averaged IOP was measured eighteen times for each eye, and the average value was used for final analysis.

Histological Analysis: The exorbital lacrimal gland, salivary and parotid glands, and whole globes were removed from mice and fixed with either 10% neutral buffered formalin or 4% paraformaldehyde (PFA) and embedded in paraffin. For general histological assessment, sections were stained with hematoxylin and eosin (H&E), or with periodic acid-Schiff (PAS) and Alcian Blue to visualize conjunctival goblet cells. Goblet cells in the bulbar and palpebral conjunctiva were quantified by two separate readers. Serial sections of tissues were stained with antibodies for anti-CD4, anti-CD8, anti-F480, anti-cytokeratin CK5 optimized by the Experimental Histology Core, NYUMC for analysis by Akoya/PerkinElmer Vectra® multispectral imaging system then counterstained with Dapi.

Lineage Tracing: For lineage tracing experiments, *Adgra3*^{creERT2} mice were crossed to the fluorescent Rosa26R-lox.STOP.lox-tdTomato lineage reporter strain (Stock No. 007909) Jackson laboratory. The transcriptional STOP was deleted by cre recombination during embryonic development (E14.5-E15.5) by delivering tamoxifen (5mg per mouse-2 doses of 2.5mg) by oral gavage to *Adgar3*$^{cre/cre}$ dams with during mid-pregnancy. Pups were delivered at E19.5-E20.5 by caesarian section to avoid problems with delivery caused by Tamoxifen and fostered by SWR/J mice. Their

tissues were harvested at 7 weeks and at 6 months to test for progenitor potency and longevity.

Tissue clearing and 3-D imaging: Lacrimal glands were excised and fixed overnight in 4% PFA then processed using a modified CUBIC (Reagent 1A) protocol Single-cell lineage tracing in the mammary gland reveals stochastic clonal dispersion of stem/progenitor cell progeny. (Davis FM et al. 2016 doi: 10.1038/ncomms13053. PMID:27779190.) Tissue was incubated in CUBIC Reagent 1A clearing solution for 4 days, rinsed 3X in PBS then immunostained for 4 days at 4C in PBST containing 10% rabbit serum and rabbit anti-K5 (Covance, PRB160P, 1:100), rinsed again then 2 days in goat anti-rabbit AlexaFluor (AF) 647 (Thermo Fisher Scientific, A21245, lot number 1805235, 1:500), rinsed 3X then cleared in CUBIC R2 for 24hrs. Cleared lacrimal tissues were imaged using a Zeiss 880 Laser Scanning inverted confocal microscope with 20X air Plan-Apochromat N.A. 0.8 M27 objective lenses.

X-gal staining: Embryos, Eyes and lacrimal glands were fixed in 4% paraformaldehyde (PFA) (Sigma-Aldrich) at room temperature (RT) for 30-60 min, rinsed 3X in X-gal rinse buffer (2 mM MgCl2, 0.1% Sodium deoxycholate, and 0.2% NP-40 in PBS) at RT, then incubated in X-gal staining solution (50 mg/ml 5-bromo-4-chloro-3-indolyl-β-D-galactopyranoside in rinse buffer containing 5 mM potassium ferricyanide, 5 mM potassium ferrocyanide) (Applichem, Cheshire, CT) at RT overnight. After staining, glands were rinsed in PBS, post-fixed in 4% PFA overnight then prepared for whole mount analysis or processed for paraffin embedding and sectioned for histological analysis.

Figure 1. Gpr125 loss induces blepharedema, blepharitis and mucus accumulation.

(A) Schematic of Gpr125 protein comprising N-terminus (N), leucine rich repeats (LRR), Immunoglobulin-like domain (Ig), hormone binding domain (HBD), GPCR autoproteolyis-inducing (GAIN) domain, 7-pass transmembrane region (TM) and cytoplasmic region (C). (**B)** Schematic of *Adgra3*. *Adgra3*$^{cre/cre}$ mice were generated by replacement of 502bp after the first codon with a creER^{T2} module. (**C)** Eye phenotype of *Adgra3*$^{cre/cre}$ and **(F)** *Adgra3*$^{lz/lz}$ mice compared to controls. **(D)** Examples of blepharedema and mucus accumulation in *Adgra3*$^{cre/cre}$ mice. **(E)** Schematic of the Gpr125-β-gal protein generated by deletion of 10 kb sequence downstream of the first TM and replacement by *lacZ*.

Figure 2. Gpr125 is expressed in eyes and eyelids.

(A) Diagram of murine eye. (**B)** Section of X-gal stained *Adgra3*$^{lz/lz}$ eye shows Gpr125-β-gal expression in the ciliary body and iris. (**C)** Intraocular pressure (IOP) (mmHg) in male (blue) and female (pink) *Adgra3*$^{lz/lz}$ and *Adgra3*$^{cre/cre}$ mice compared to their respective FVBN and B6 controls. Each bar represents the mean ± SEM on 6-14 mice/group. ns, not significant. (**D)** Fluorescein stained corneas in *Adgra3*$^{cre/cre}$ and control mice. n=3 (**E)** Schematic of tear film. (**F)** Eyelid sections stained with alcian blue AB/PAS show goblet cells in *Adgra3*$^{cre/cre}$ and control mice. n=23. **(G,H)** H/E of meibomian glands and **(H)** immunostained with antibodies: F480, CD4,CD8, CK5 and DAPI to detect macrophages, T-helper, cytotoxic T cells, cytokeratin 5 and nuclei respectively in *Adgra3*$^{cre/cre}$ mice. Control *Adgra3*$^{+/+}$ in S1A. **I)** X-gal stained whole mounts of P10 eyelids from *Adgra3*$^{lz/lz}$ mice with meibomian glands (arrowheads) devoid of Gpr125.Scale bar 100μm. n=3.

Figure 3. Loss of Gpr125 leads to abnormal lacrimation and inflammatory infiltration of the lacrimal glands

(A) Increased tear production observed in *Adgra3*$^{cre/cre}$ and *Adgra3*$^{lz/lz}$ male (blue) and female (pink) mice compared to controls. Each bar represents the mean ± SEM on 6-32 mice. **** $p<0.0001$, **, $p<0.05$ value significant; ns, not significant. **(B)** H/E section of lacrimal gland from *Adgra3*$^{cre/cre}$ mice shows foci of infiltration (arrows). Control *Adgra3*$^{+/+}$ in S1C. **(C-G)** Immunofluorescence of lacrimal gland co-stained for **(D)** CK5, **(E)** macrophages, **(F)** T-helper, **(G)** cytotoxic T cells. **(H)** *Adgra3*$^{cre/cre}$ female with lacrimal mass H/E stained in **(I,J)**.**(K)** Immunofluorescence analysis of boxed region in **I**. Scale bar 100μm.

Figure 4. Gpr125 cells, located at ductal tips during development, function as lacrimal myoepithelial progenitors.

A) t-SNE plot of cells clusters within E16 lacrimal glands (10). Zoomed images of E16 epithelial compartment (boxed region) show cells expressing Adgra3 mRNA also express myoepithelial markers, Keratin14 and Sox10 but not luminal markers Keratin19 or Aquaporin5. **B)** Gpr125-β-gal expression in embryos. **C)** Strategy for tracing the lineage of Gpr125-positive cells in E14.5-E15.5 embryos carrying the *Rosa26*.lox.STOP.lox.TdTomato reporter by tamoxifen injection of pregnant *Adgra3*$^{cre/cre}$ dams. 3D-confocal images of lacrimal glands from mice at **(D)** 7 weeks and **(E)** 6 months showing tdT expression in elongated myoepithelial cells along the basal border of ducts

and stellate cells enmeshing acini colocalized with myoepithelial marker (CK5). Scale bar 50μm.n=3.

Figure S1.

(A,B) Meibomian gland immunostained with antibodies: F480, CD4, CD8, CK5 and DAPI to detect macrophages, T-helper, cytotoxic T cells, cytokeratin 5 and nuclei respectively in control *Adgra3*$^{+/+}$ and *Adgra3*$^{cre/cre}$ mice. **(C,D)**H/E section of lacrimal gland from control *Adgra3*$^{+/+}$ and *Adgra3*$^{cre/cre}$ mice. Scale bar 100μm.

Figure 1

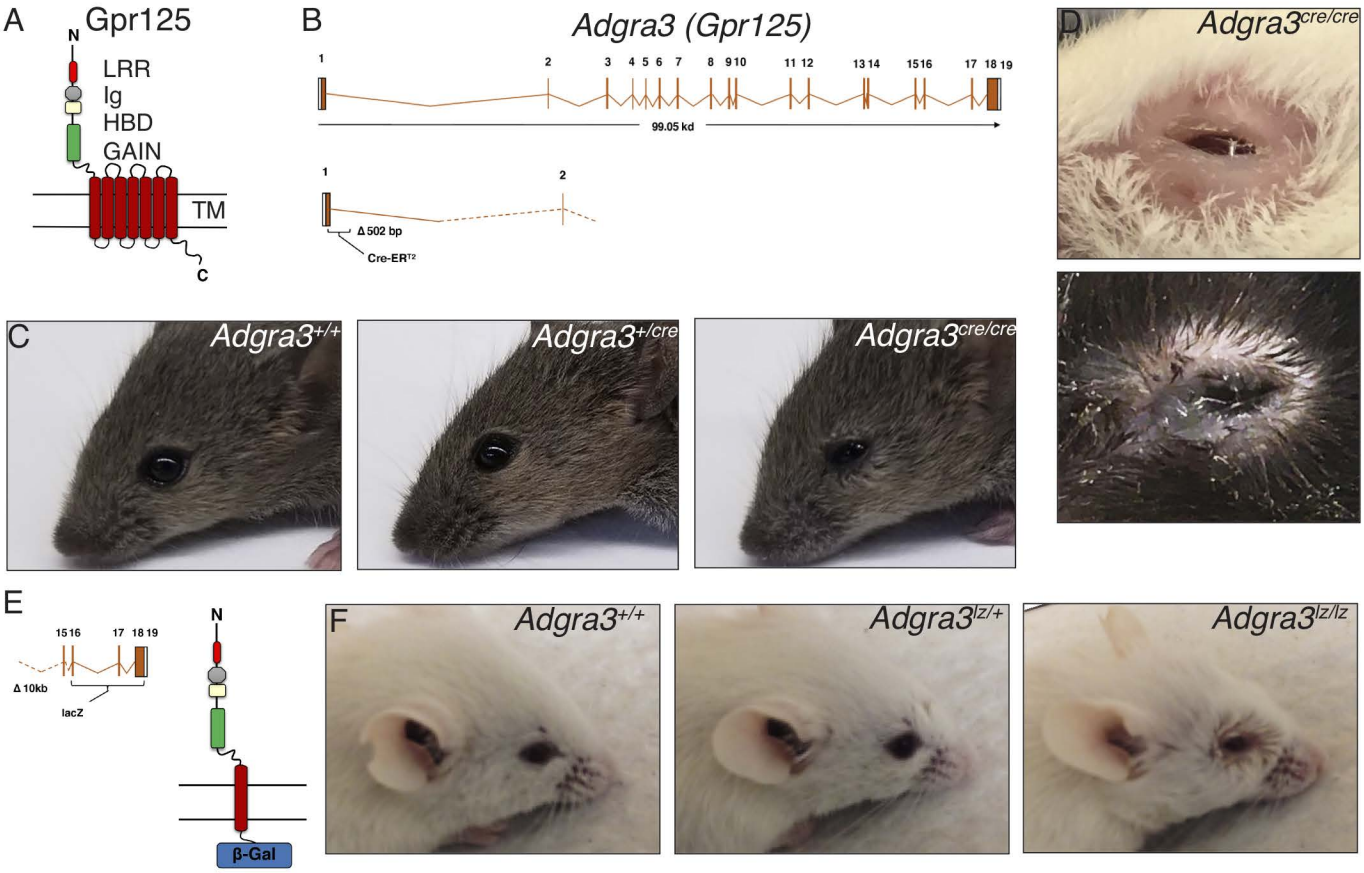
A
Gpr125
N
LRR
Ig
HBD
GAIN
TM
C
B
Adgra3 (Gpr125)
1
2
3
4 5 6
7
8
9 10
11 12
13 14
15 16
17
18 19
99.05 kd
1
2
Δ 502 bp
Cre-ERT2
D
Adgra3cre/cre
C
Adgra3+/+
Adgra3+/cre
Adgra3cre/cre
E
15 16
17
18 19
Δ 10kb
lacZ
N
β-Gal
F
Adgra3+/+
Adgra3lz/+
Adgra3lz/lz

Figure 2

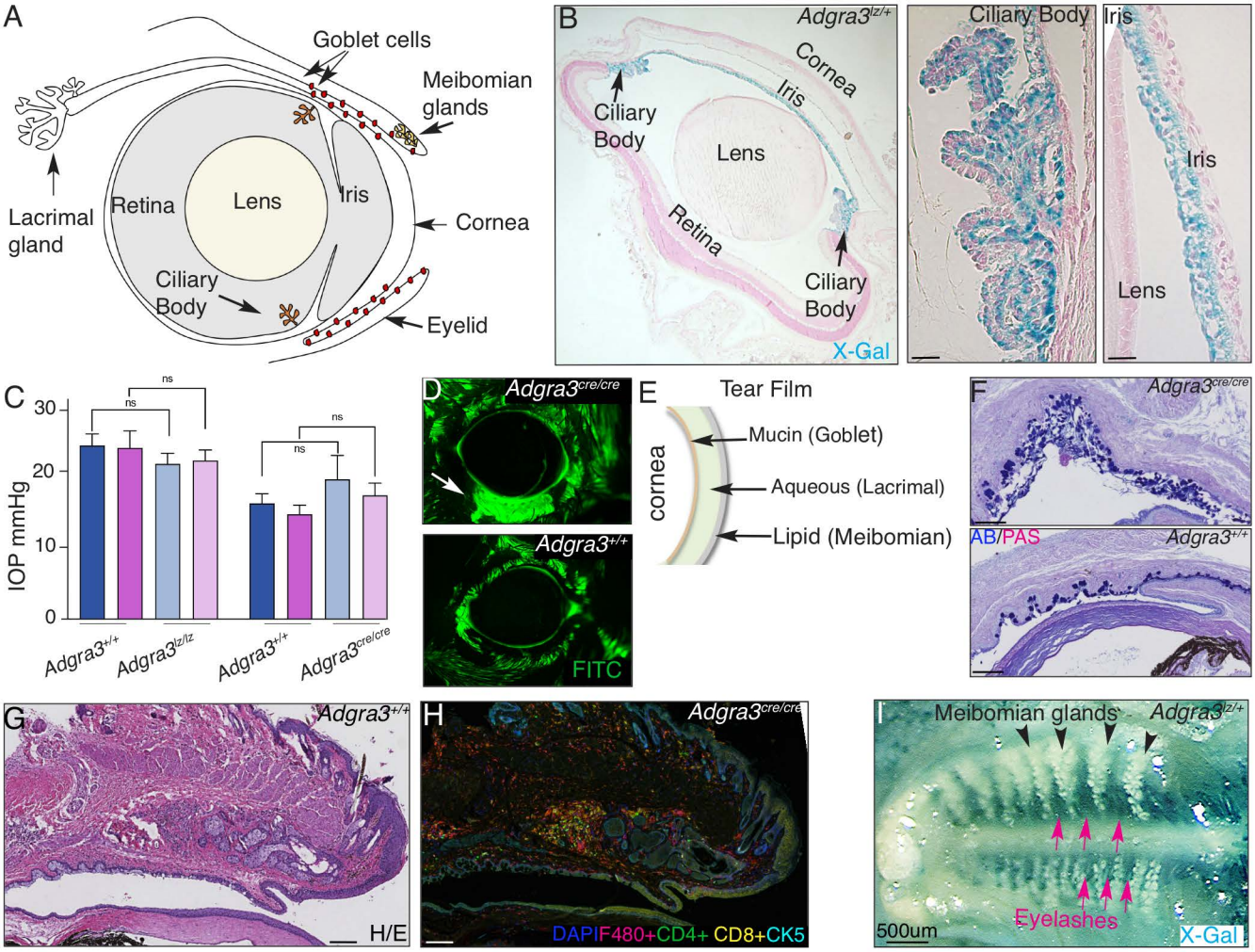
A
Goblet cells
Meibomian glands
Lacrimal gland
Retina
Lens
Iris
Cornea
Ciliary Body
Eyelid
B
Adgra3lz/+
Cornea
Iris
Ciliary Body
Lens
Retina
Ciliary Body
X-Gal
Ciliary Body
Iris
Iris
Lens
C
IOP mmHg
30
20
10
0
ns
ns
ns
ns
Adgra3+/+
Adgra3lz/lz
Adgra3+/+
Adgra3cre/cre
D
Adgra3cre/cre
Adgra3+/+
FITC
E
Tear Film
cornea
Mucin (Goblet)
Aqueous (Lacrimal)
Lipid (Meibomian)
F
Adgra3cre/cre
AB/PAS
Adgra3+/+

G
Adgra3+/+
H/E
H
Adgra3cre/cre
DAPIF480+CD4+ CD8+CK5
I
Meibomian glands
Adgra3lz/+
Eyelashes
500um
X-Gal

Figure 3

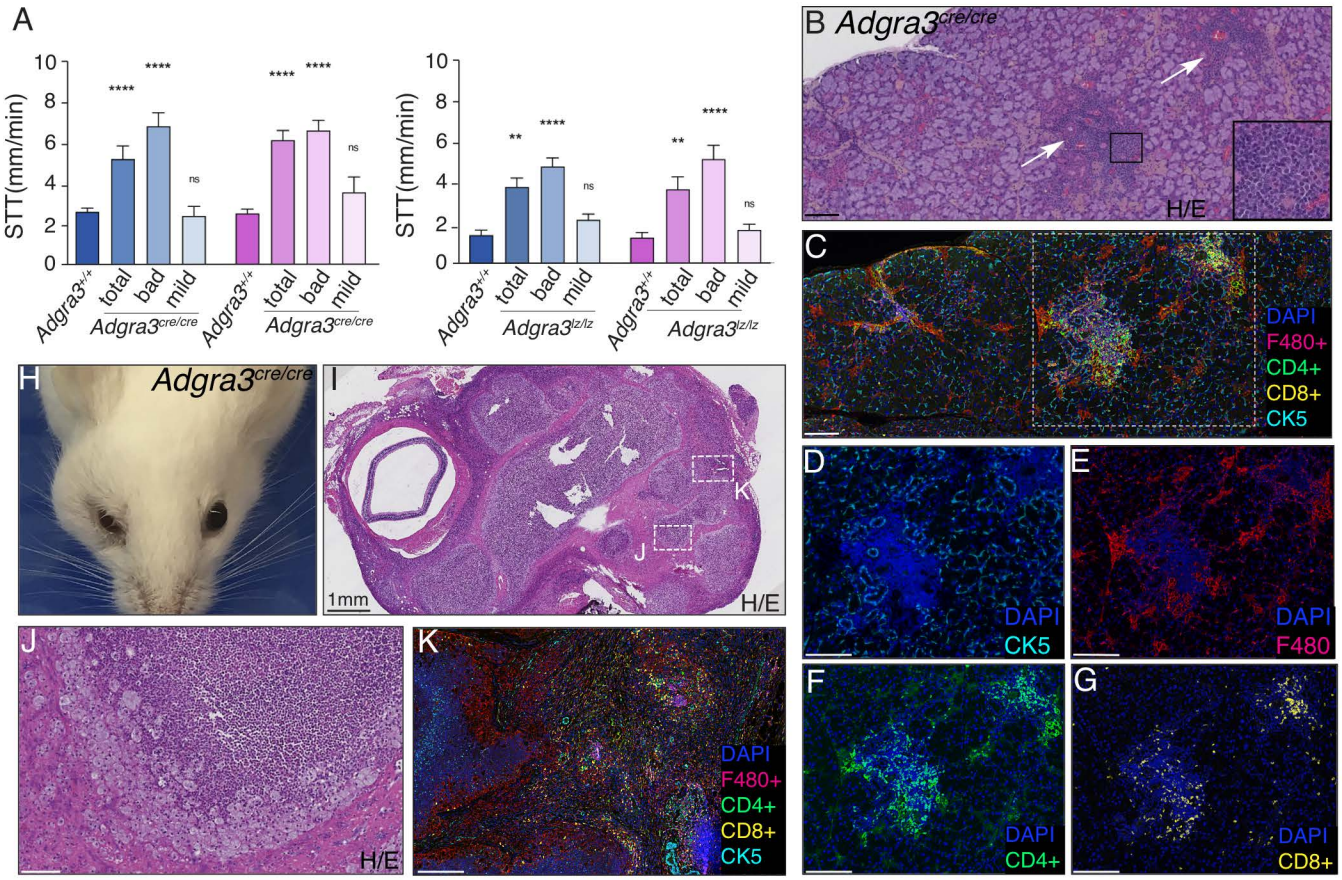
A
STT(mm/min)
10
8
6
4
2
0
****
****
****
****
ns
ns
**
**
Adgra3+/+
total
bad
mild
Adgra3cre/cre
Adgra3lz/lz
B Adgra3cre/cre
H/E
C
DAPI
F480+
CD4+
CD8+
CK5
D
E
F
G
H
Adgra3cre/cre
I
1mm
H/E
J
K

Figure 4

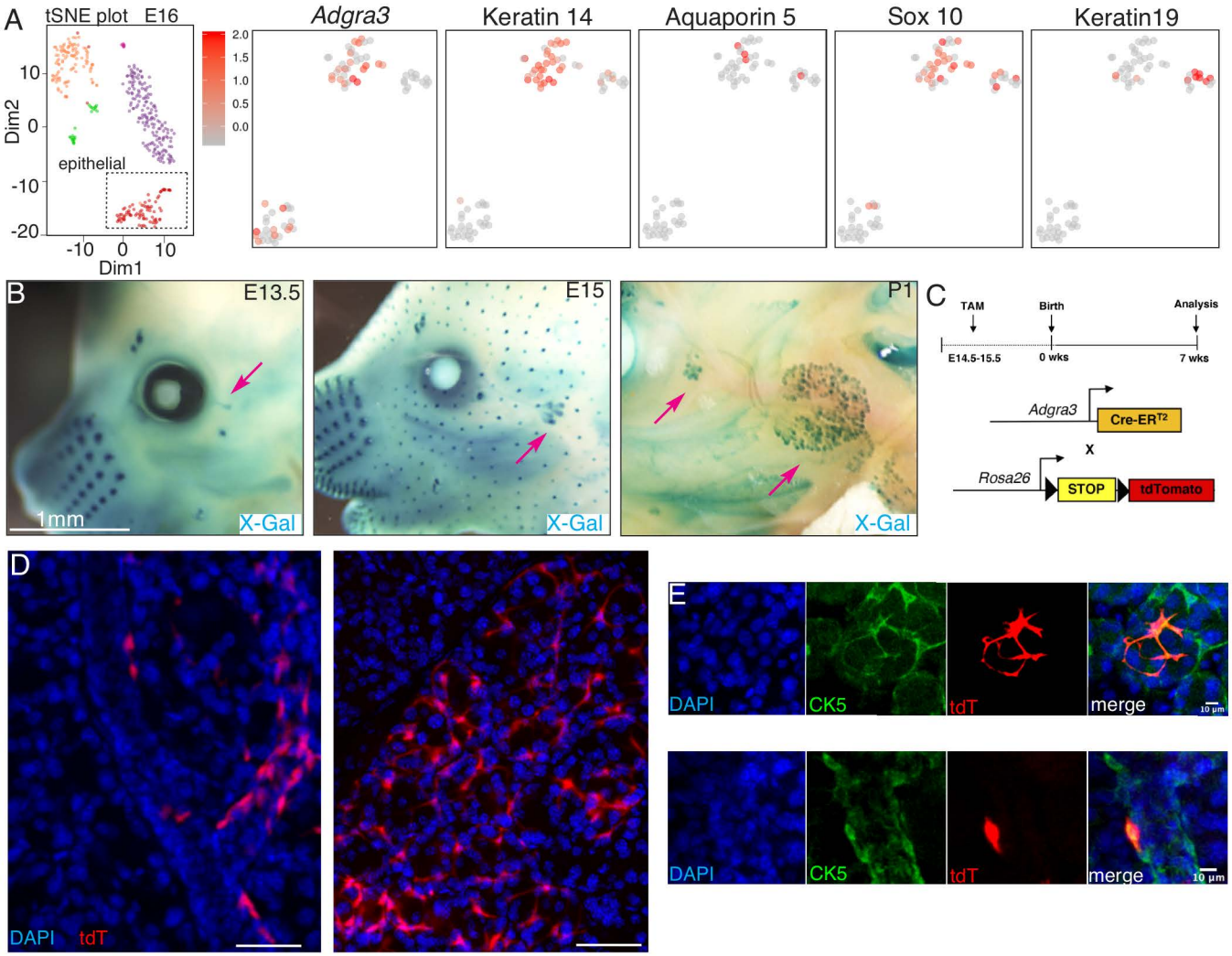
A
tSNE plot E16
Dim2
Dim1
epithelial
2.0
1.5
1.0
0.5
0.0
Adgra3
Keratin 14
Aquaporin 5
Sox 10
Keratin19
B
E13.5
E15
P1
1mm
X-Gal
C
TAM
Birth
Analysis
E14.5-15.5
0 wks
7 wks
Adgra3
Cre-ER^{T2}
X
Rosa26
STOP
tdTomato
D
DAPI
tdT
E
DAPI
CK5
tdT
merge
10 µm

Figure S1

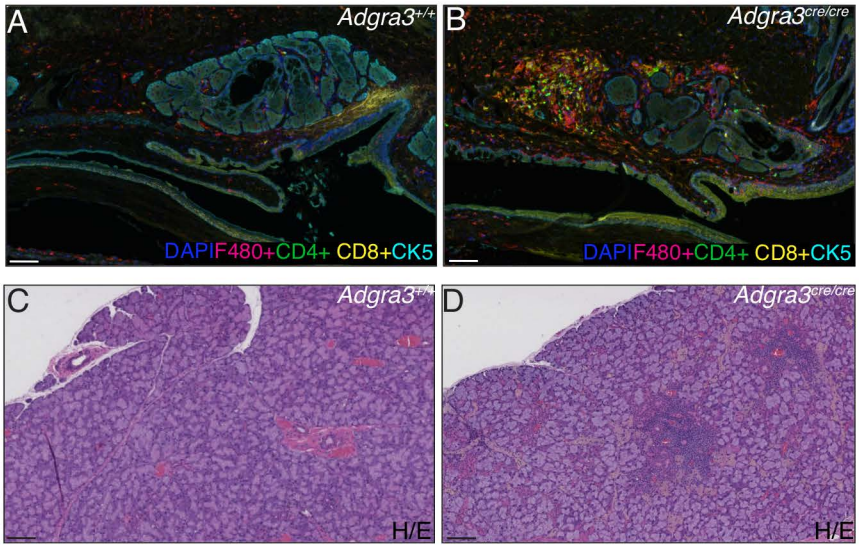
A
Adgra3+/+
DAPIF480+CD4+ CD8+CK5
B
Adgra3cre/cre
DAPIF480+CD4+ CD8+CK5
C
Adgra3+/+
H/E
D
Adgra3cre/cre
H/E